PHYSICAL REVIEW B **69**, 220402(R) (2004)

Universal scaling at field-induced magnetic phase transitions

Omid Nohadani,[1,*] Stefan Wessel,[2] B. Normand,[3] and Stephan Haas[1]
[1]*Department of Physics and Astronomy, University of Southern California, Los Angeles, California 90089-0484, USA*
[2]*Institut für Theoretische Physik, ETH-Hönggerberg, CH-8093 Zürich, Switzerland*
[3]*Département de Physique, Université de Fribourg, CH-1700 Fribourg, Switzerland*
(Received 5 March 2004; published 7 June 2004)

We study field-induced magnetic order in cubic lattices of dimers with antiferromagnetic Heisenberg interactions. The thermal critical exponents at the quantum phase transition from a spin liquid to a magnetically ordered phase are determined from stochastic series expansion quantum Monte Carlo simulations. These exponents are independent of the interdimer coupling ratios, and converge to the value obtained by considering the transition as a Bose-Einstein condensation of magnons, $\alpha_{\mathrm{BEC}}=\frac{3}{2}$. The scaling results are of direct relevance to the spin-dimer systems $TlCuCl_3$ and $KCuCl_3$, and explain the broad range of exponents reported for field-induced ordering transitions.

DOI: 10.1103/PhysRevB.69.220402 PACS number(s): 75.10.Jm, 75.40.Cx, 75.40.Gb

A quantum spin liquid is characterized by a finite magnetic correlation length, which is inversely proportional to the energy gap Δ_0 between the singlet ground state and the lowest triplet excitation. Application of an external magnetic field causes a linear reduction of Δ_0 by the Zeeman effect. At zero temperature there is a field-induced quantum phase transition (QPT), at a lower critical field $h_{c1}\equiv g\mu_{\mathrm{B}}H_{c1}=\Delta_0$, from the spin liquid to a magnetically ordered state. In this phase the uniform magnetic polarization then rises continuously from zero to saturation at a second critical field h_{c2}. Such transitions have been observed in a variety of quantum antiferromagnets, including $Cu_2(C_5H_{12}N_2)_2Cl_4$,[1] $KCuCl_3$,[2,3] and $TlCuCl_3$,[2,4,5] which consist of weakly coupled, low-dimensional structural units such as spin ladders or dimers. In the ordered phase, the uniform magnetization is accompanied by a long-ranged antiferromagnetic (AF) spin ordering in the plane perpendicular to the field, which persists up to a finite transition temperature T_c determined by the smallest coupling constant between the magnetic structural units.

The compounds $KCuCl_3$ and $TlCuCl_3$ provide an excellent illustration of the field-induced QPT from a dimer spin liquid to a three-dimensional (3D) ordered phase. These systems consist of dimer units formed by pairs of $S=1/2$ Cu^{2+} ions with significant interdimer superexchange interactions in all three spatial directions.[3,4] Because these interactions are considerably weaker in $KCuCl_3$ than in $TlCuCl_3$, the magnon modes of the former have a narrow band and a large spin gap ($\Delta_0=2.6$ meV), while the latter represents a wide-band system with a small gap ($\Delta_0=0.7$ meV). The wave vector $\mathbf{Q}$ of the 3D AF order is the location in momentum space of the band minimum, Δ_0, of the triplet magnon excitations, which are gapped in the disordered phase. The field-induced QPT may be regarded as a condensation of magnons in the lowest triplet branch, which becomes the gapless excitation, or Goldstone mode, corresponding to rotations of the staggered magnetic moment about the field axis and reflecting the broken symmetry of the system.[6] The continuous evolution of the ordered moments is then equivalent to a field-dependent density of condensed magnons, and the magnetic field represents an experimentally accessible tuning parameter for the QPT.

The suggestion that this transition may be described as the Bose-Einstein condensation (BEC) of hard-core bosons[7] has motivated extensive experimental and theoretical studies of the critical properties of such systems. Particular attention is given to the scaling exponent α which determines the power-law dependence

$$T_c(h)\propto|h-h_c|^{1/\alpha} \tag{1}$$

of the ordering temperature on the field h in the vicinity of the QPT's at $h_c\equiv h_{c1}$ and h_{c2}. Different experimental studies indicate that the precise value of this exponent at h_{c1} depends on the material as well as on the measuring technique. The exponents $\alpha\approx 1.8-2.3$ extracted from experimental studies of $KCuCl_3$ and $TlCuCl_3$ (Refs. 2–5) are all larger than the value $\alpha_{\mathrm{BEC}}=3/2$ obtained from the BEC scenario for 3D systems in which the magnon modes have quadratic dispersion at the band minimum.[7] The analytic bond-operator approach, applied with the parameters of $KCuCl_3$ and $TlCuCl_3$, also yields the respective values 2.6 and 1.8,[8] while recent quantum Monte Carlo simulations for weakly coupled dimers,[9] suggest that $\alpha\sim 2.3$. In both experiments and simulations, precise extraction of the critical exponent is complicated by the fact that typically only rather few data points are available close to the QPT. In addition, the exponent may not reflect universal critical behavior if the temperature exceeds an (unknown) upper bound for the validity of the BEC approach. However, it is also possible that the scaling behavior is simply not universal, in that the exponent depends on certain system parameters, most notably the strength of the interdimer interactions.

To analyze the scaling behavior associated with field-induced magnetic order, we study a Heisenberg model of coupled spin-1/2 dimers with the Hamiltonian

$$H=\sum_{\langle i,j\rangle} J_{ij}\mathbf{S}_i\cdot\mathbf{S}_j-h\sum_i S_i^z. \tag{2}$$

The AF coupling constants J and J' between nearest-neighbor sites i and j denote, respectively, the intradimer and interdimer superexchange interactions for the cubic geometry of which a planar section is illustrated in the inset of Fig.

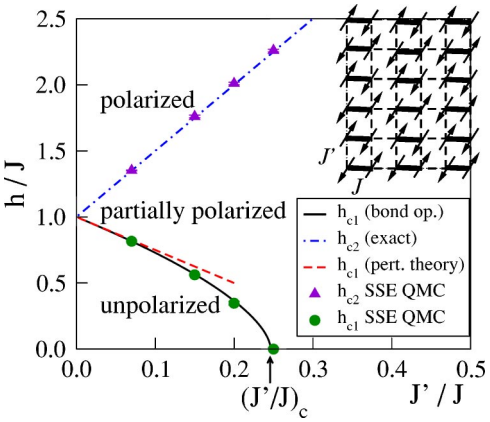

FIG. 1. (Color online) Phase diagram of 3D AF coupled dimers in a magnetic field. The solid line represents h_{c1} and the dot-dashed line h_{c2}. Circles and triangles are zero-temperature fits obtained from SSE QMC results. Inset: one layer of coupled dimers.

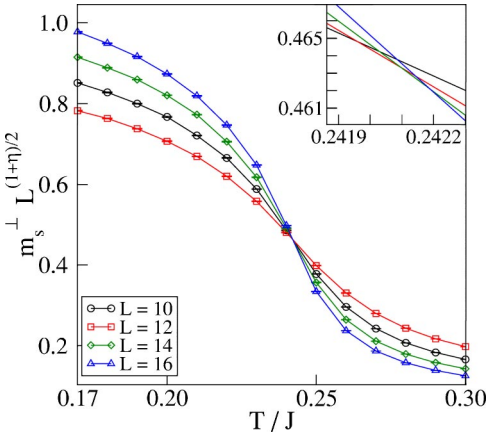

FIG. 2. (Color online) Scaled staggered magnetization at constant field $h=0.8J$ and interdimer coupling $J'=0.25J$, for a range of system sizes. T_c is determined from the intersection of the four curves (main panel), and its error from the extremal intersection points (inset).

1. Because the $K/TlCuCl_3$ structure has no magnetic frustration, the AF cubic dimer system is expected to illustrate the same generic similarities and differences between large- and small-gap systems as those obtained in the experimental studies to date.

We take as the order parameter the component of staggered magnetization perpendicular to the applied field,

$$m_s^{\perp} = \sqrt{\frac{S_s^{\perp}}{L^3}} \tag{3}$$

where L denotes the linear system size and $S_s^{\perp}$ the perpendicular staggered structure factor defined as

$$S_s^{\perp} = \frac{1}{L^3} \sum_{\langle i,j \rangle} (-1)^{i+j} \langle S_i^x S_j^x \rangle. \tag{4}$$

This quantity is calculated using the stochastic series expansion quantum Monte Carlo (SSE QMC) method of Refs. 10 and 11. The staggered structure factor is sampled ''on the run'' as loop updates are constructed,[12] with implementation of the directed-loop algorithm[13] to minimize bounce probabilities within a loop. This procedure yields a significantly higher sampling efficiency than the conventional operator-loop update: close to criticality ($J' \geqslant 0.2J$ and $h \leqslant 0.7J$), where the maximum number of runs is required, autocorrelation times are reduced by factor of up to 8. Simulations were performed for cubic clusters of up to 8000 spins, and for temperatures down to $T=0.03J$, except at very small J' where smaller values are readily obtainable.

The zero-temperature phase diagram of the coupled-dimer system is shown in Fig. 1. In the absence of a magnetic field the computed quantum critical point, separating the spin-disordered, dimer valence-bond-solid (DVBS) phase from the ordered AF phase, occurs at $(J'/J)_c = 0.255(5)$. Both phases are unpolarized at $h=0$. Their elementary excitations have the same fundamental difference as for the field-induced QPT, except that the coupling-induced ordered phase has two Goldstone modes [associated with the broken O(3) symmetry] corresponding to the phase fluctuations of the staggered moment. The uniform magnetization varies continuously with applied field from zero in the DVBS phase ($h \leqslant h_{c1}$) to full polarization at $h \geqslant h_{c2}$. In the ordered phase the staggered moment first increases with h beyond h_{c1} (also for $J' > J'_c$) before falling continuously to zero at h_{c2}.

The values of h_{c2} obtained from SSE QMC simulations (triangles in Fig. 1) coincide with the exact result, which is classical because quantum fluctuations are entirely suppressed in the saturated regime. By contrast, quantum corrections are essential to the determination of h_{c1}, where a straightforward perturbative expansion (dashed line) departs from the numerical data (circles) for $J' > 0.08J$. However, the self-consistent bond-operator solution (solid line) provides an accurate description of the numerical results at all interdimer couplings, including those close to J'_c. The quantitative success of this theory for $KCuCl_3$ and $TlCuCl_3$ may be ascribed to the 3D nature of the ordered phase.[6]

Turning to finite-temperature properties, the transition temperatures for the ordered phase are determined by finite-size scaling of the order parameter $m_s^{\perp}$. Figure 2 illustrates this procedure: in 3D and at the critical temperature, $m_s^{\perp}$ at fixed field is expected to obey the scaling relation $m_s^{\perp} \propto L^{(1-z-\eta)/2}$, where the dynamical exponent z is zero for a thermal transition.[14] For a system with spontaneous breaking of the residual O(2) symmetry the correlation exponent can be taken from the classical 3D XY model, for which $\eta = 0.0381(2)$.[15] In the vicinity of the critical temperature, T_c, the scaled $m_s^{\perp}$ is linear in T,[16] and the intersection of the curves obtained for different system sizes L determines T_c at all fields $h \in [h_{c1}, h_{c2}]$ for a given interdimer coupling J'. Magnification of the intersection region (inset Fig. 2) reveals a set of intercepts within a temperature window $\Delta T \sim 0.0005J$, which determines $T_c(h)$ to very high accuracy.[17]

Figure 3 shows the critical temperatures $T_c(h)$ obtained for four interdimer coupling ratios, $(J'/J) = 0.07$, 0.15, 0.20, and 0.25,[17] which span the range from narrow-band, large-gap systems to the wideband, small-gap paradigm. Each cou-

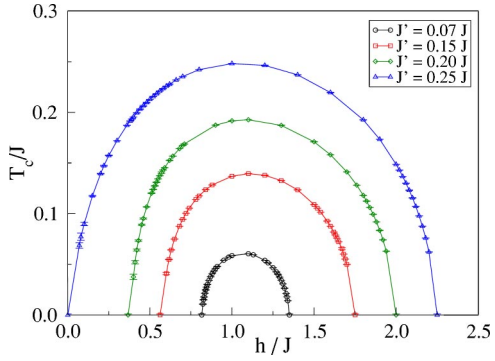

FIG. 3. (Color online) Critical temperature for field-induced order in 3D systems of coupled dimers for a range of values of J'. Symbols are taken directly from finite-size scaling of SSE QMC simulations, except for the $T=0$ points which are extracted from fits of $T_c(h)$. Solid lines are guides to the eye.

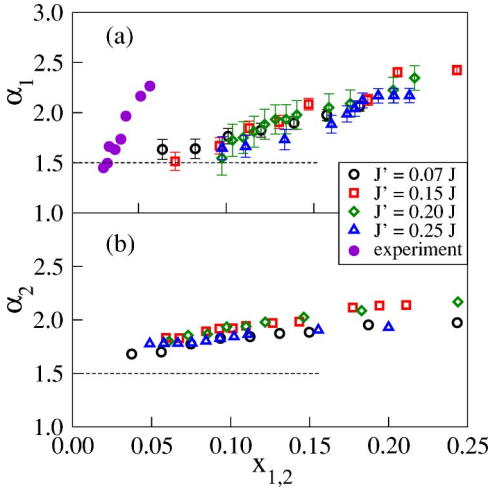

FIG. 4. (Color online) Critical exponents α_1 at h_{c1} (a) and α_2 at h_{c2} (b), shown as a function of the fitting range x (see text). Filled circles in (a) are experimental data from Ref. 5. Dashed lines mark the result of the BEC description.

pling ratio corresponds to a vertical section in Fig. 1, where the values of h_{c1} and h_{c2} in Fig. 3 mark the boundaries of the ordered phase; h_{c1} vanishes for $J'>J'_c$. The weak asymmetry of $T_c(h)$ about the midpoint field, $(h_{c1}+h_{c2})/2$, becomes more pronounced for stronger couplings due to changes at the extrema of the magnon dispersion relations determining the transitions.[6] The values of $T_c(h)$ obtained by the systematic scaling procedure confirm, within the error bars, the location of the dips in uniform magnetization reported in previous numerical studies,[9] and used to construct the experimental phase diagram of $TlCuCl_3$.[4]

We now focus on the scaling properties of $T_c(h)$ close to h_{c1} and h_{c2}. The scaling exponent α in Eq. (1) is obtained by fitting the data shown in Fig. 3 with h_c and α as free parameters. We fit this data within a varying window, i.e., for given J'/J we define

$$x_1(h)=\frac{h-h_{c1}}{h_{c2}-h_{c1}}, \quad x_2(h)=\frac{h_{c2}-h}{h_{c2}-h_{c1}}, \tag{5}$$

as normalized measures of the proximity to the lower and upper critical fields. Using a minimum of six data points in a given window x_1 or x_2, the exponents α_1 and α_2 are then determined by nonlinear curve fitting. The fitted exponents are crucially dependent both on the number of points and on the exact critical field (Fig. 1).[18]

The dependence on window size x_1 of the exponent α_1 is shown in Fig. 4(a). A first, unambiguous conclusion from Fig. 4 is that the fitted exponents become smaller as the window size is decreased, and, in particular, a large window leads to overestimation of α_1. It is also clear that the extrapolated values approach $\alpha_{\mathrm{BEC}}=\frac{3}{2}$. Higher exponents suggested by previous results are seen to be a product of the fitting procedure employed, and are in fact consistent with the BEC scenario at the transition [Fig. 4(a)]. Most remarkably, the lines for all interdimer couplings not only scale to the same limit but do so with the same slope for all x, demonstrating that the critical behavior is truly universal for all ratios of bandwidth to spin gap. We have performed the same varying-window fit to the experimental data for $T_c(h)$ in $TlCuCl_3$:[5,18] the results shown in Fig. 4(a) demonstrate a similar sensitivity to window size and consistency with BEC scaling only close to the QPT. The nonuniversal behavior of the exponent α_1 beyond the BEC regime is naturally different from the numerical data because of differences in the geometry of the magnetic system.

Results for α_2 are shown in Fig. 4(b), and are again consistent with the BEC description as $x_2\to 0$. Here the spread of data points is smaller than for $\alpha_1(x_1)$, and the slope of $\alpha_2(x_2)$ is less steep. These results may be attributed to the less significant role of quantum fluctuations near h_{c2}, which leads to smaller deviations from a mean-field scaling regime.

It must be emphasized that the universal scaling behavior is obtained only for very narrow windows, meaning very low temperatures. From Fig. 4, our results may be interpreted as indicating that BEC scaling emerges below a temperature $T\sim 0.5J'$ in the vicinity of h_{c1}, but that such an upper bound cannot be determined for h_{c2}, where the BEC regime is approached only as $T\to 0$. At both critical fields, the physical origin of departure from universal scaling is found in the approximations inherent to the BEC description,[7] primarily a temperature-driven renormalization of the quasiparticle effective mass (curvature in reduction at the band minimum) and of the effective chemical potential (band narrowing with concomitant increase in spin gap).

In summary, we have used an unbiased numerical technique to study field-induced magnetic ordering transitions in cubic systems of antiferromagnetically coupled dimers. The phase diagram contains two quantum critical lines, $h_{c1}(J'/J)$ and $h_{c2}(J'/J)$. Both transitions are continuous, as is the variation in physical properties of the intermediate AF phase, as a function of applied magnetic field. The critical scaling exponents α extracted for the transition temperature close to h_{c1} and h_{c2} are found to be independent of the interdimer coupling ratio, demonstrating that, despite large quantitative differences in their magnon dispersion relations, the physical properties of the coupled-dimer systems $KCuCl_3$ and $TlCuCl_3$ display the same universal scaling behavior. The

values of α are consistent with a description of the ordering transitions as the Bose-Einstein condensation of magnon excitations, $\alpha_{\mathrm{BEC}}=\frac{3}{2}$. However, this regime is obtained only in the limit of temperatures very small compared to the interdimer coupling. Finally, the fits to the exponents were shown to depend sensitively on the window size, with the consequence that α is easily overestimated. This result offers an explanation for the wide range of scaling exponents reported in the literature.

We thank F. Alet, A. Honecker, A. Läuchli, M. Matsumoto, T. Roscilde, A. Sandvik, M. Sigrist, H. Tanaka, and M. Troyer for helpful discussions. We acknowledge financial support from the NSF, under Grant No. DMR-0089882, and from the Swiss NSF. Computational support was provided by the USC Center for High Performance Computing and Communications, by the NERSCC, and by Asgard at ETH Zürich.

*Electronic address: nohadani@usc.edu

[1] G. Chaboussant, P.A. Crowell, L.P. Levy, O. Piovesana, A. Madouri, and D. Mailly, Phys. Rev. B **55**, 3046 (1997); M.B. Stone, Y. Chen, J. Rittner, H. Yardimci, D.H. Reich, C. Broholm, D.V. Ferraris, and T. Lectka, *ibid.* **65**, 064423 (2002); M. Mito, H. Akama, T. Kawae, K. Takeda, H. Deguchi, and S. Takagi, *ibid.* **65**, 104405 (2002).

[2] W. Shiramura, K. Takatsu, H. Tanaka, K. Kamishima, M. Takahashi, H. Mitamura, and T. Goto, J. Phys. Soc. Jpn. **66**, 1900 (1997).

[3] T. Kato, K. Takatsu, H. Tanaka, W. Shiramura, M. Mori, K. Nakajima, and K. Kakurai, J. Phys. Soc. Jpn. **67**, 752 (1998); A. Oosawa, T. Takamasu, K. Tatani, H. Abe, N. Tsujii, O. Suzuki, H. Tanaka, G. Kido, and K. Kindo, Phys. Rev. B **66**, 104405 (2002).

[4] A. Oosawa, M. Ishii, and H. Tanaka, J. Phys.: Condens. Matter **11**, 265 (1999); N. Cavadini, G. Heigold, W. Henggeler, A. Furrer, H.-U. Güdel, K. Krämer, and H. Mutka, Phys. Rev. B **63**, 172414 (2001); Ch. Rüegg, N. Cavadini, A. Furrer, H.-U. Güdel, K. Krämer, H. Mutka, A. Wildes, K. Habicht, and P. Vorderwisch, Nature (London) **423**, 62 (2003).

[5] H. Tanaka, A. Oosawa, T. Kato, H. Uekusa, Y. Ohashi, K. Kakurai, and A. Hoser, J. Phys. Soc. Jpn. **70**, 939 (2001).

[6] M. Matsumoto, B. Normand, T.M. Rice, and M. Sigrist, Phys. Rev. Lett. **89**, 077203 (2002).

[7] T. Giamarchi and A.M. Tsvelik, Phys. Rev. B **59**, 11 398 (1999); T. Nikuni, M. Oshikawa, A. Oosawa, and H. Tanaka, Phys. Rev. Lett. **84**, 5868 (2000).

[8] M. Matsumoto (private communication).

[9] S. Wessel, M. Olshanii, and S. Haas, Phys. Rev. Lett. **87**, 206407 (2001).

[10] A.W. Sandvik, Phys. Rev. B **59**, R14 157 (1999).

[11] A.W. Sandvik, Phys. Rev. B **56**, 11 678 (1997).

[12] A. Dorneich and M. Troyer, Phys. Rev. E **64**, 066701 (2001).

[13] O.F. Syljuåsen and A.W. Sandvik, Phys. Rev. E **66**, 046701 (2002). Because the Hamiltonian is isotropic in spin space and nonvanishing magnetic fields are considered, these loops are not entirely bounce-free.

[14] M. Troyer and M. Imada, in *Computer Simulations in Condensed Matter Physics X*, edited by D.P. Landau *et al.* (Springer-Verlag, Heidelberg, 1997).

[15] M. Hasenbusch and T. Török, J. Phys. A **32**, 6361 (1999).

[16] A.W. Sandvik, Phys. Rev. Lett. **80**, 5196 (1998).

[17] We have performed simulations for system sizes $L\leqslant 20$. However, data obtained for $L=20$ neither improve the results nor reduce the error bars appreciably, and we have restricted production runs to system sizes $L\leqslant 16$.

[18] The errors $\Delta\alpha_1$ in Fig. 4(a) are due to uncertainties in h_c1, which demand a two-parameter fit. Because h_c2 is known, α_2 may be obtained from a single-parameter fit, resulting in smaller uncertainties $\Delta\alpha_2$ [smaller than the symbol sizes in Fig. 4(b)]. The error quoted for the measured critical field Ref. 5, $h_c1=5.7(1)$ T, yields a 25% error in α_1 which is not shown in Fig. 4. The relevant h_c2 is taken from Ref. 6.